Optical emission study of ion composition in an inductively coupled oxygen plasma

Nathaniel Ly

Under the supervision of:

Amy Wendt and John Boffard, University of Wisconsin—Madison

July 31st, 2015

Abstract:

The success of ion implantation to precisely modify substrate properties is dependent on controlling the incident ion energies to achieve the desired depth of the implanted ions. Oxygen plasmas generally contain both O^+ and O_2^+ ions, and in plasma immersion ion implantation (PIII) of oxygen, the two will produce different concentration depth profiles due to their different energy/mass ratios. Predicting the overall profile thus requires knowledge of the relative fluxes of the two ion species. Here we investigate the feasibility of using non-invasive optical emission spectroscopy (OES) to monitor O^+ and O_2^+ abundances in an inductively-coupled oxygen plasma. Measurements of O, O_2, O^+, and O_2^+ emission intensities were made as a function of pressure (1-30 mTorr) and power (500-2000 W). O^+ emissions were very weak for all conditions examined. Emissions from both ion species peaked at the lowest pressures and at the highest power levels, but the O^+/ O_2^+ emission ratio varied little with plasma conditions.

Introduction:

Ion implantation of oxygen is of interest for the formation of thin electrically insulating layers. The success of ion implantation to precisely modify substrate properties is dependent on controlling the incident ion energies to achieve the desired depth of the implanted ions. In PIII, incident ion energy is controlled by means of the bias voltage periodically applied to the substrate electrode. The application of the bias voltage creates a high voltage sheath adjacent to the substrate, and the sheath electric field accelerates plasma ions toward the substrate at normal incidence. Oxygen plasmas generally contain both O^+ and O_2^+ ions, and in PIII of oxygen, the two will produce different concentration depth profiles due to their different energy/mass ratios when they arrive at the substrate. Prediction of the overall concentration depth profile thus requires knowledge of the relative fluxes to the substrate of the two ion species. If the relative fluxes of the two were found to vary significantly with plasma conditions, a method of further controlling the implantation process can be envisioned, in which plasma conditions could be selected that would produce either O^+ or O_2^+ as the dominant implantation ion.

The study presented here constitutes only a first step toward the goals articulated above; we investigate the feasibility of using non-invasive optical emission spectroscopy (OES) to monitor O^+ and O_2^+ abundances in oxygen inductively-coupled plasmas, as a probe, albeit an indirect one, related to the relative fluxes of the two species. The emission intensities we monitor for O^+ and O_2^+ are functions of the concentrations of the neutral species involved as well as the electron

density and energy distribution function and thus are not a direct measure of either the gas phase concentrations of the ion species or their fluxes at the substrate surface. Nevertheless, changes in emission intensity ratio for the two can be expected as their concentrations change with plasma conditions, and it thus provides a qualitative indirect monitor of changes in the relative abundances of the two types of ions.

Spectra of a research grade (99.9999% purity) oxygen plasma were taken over a range of operating parameters in an rf inductively coupled O_2 plasma. The input power ranged from 500 W to 2000 W in 500 W increments and the pressures sampled ranged from 1 mTorr to 30 mTorr. Spectral intensities of O, O_2, O^+, and O_2^+ were detected with a photomultiplier tube (PMT).

Experimental Setup:

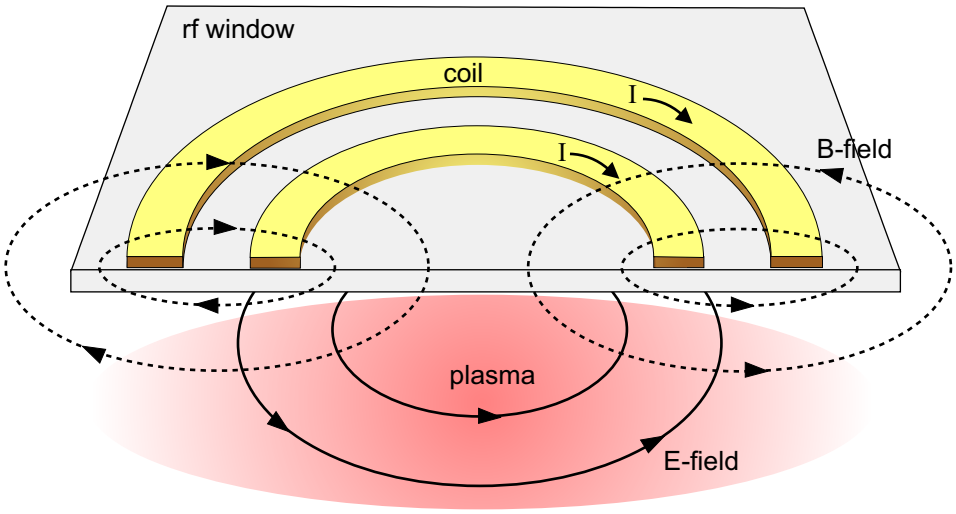

Figure 1: Cross-sectional view of planar inductively coupled rf plasma, showing the external induction antenna, quartz vacuum window and fields induced by antenna currents.

An inductively coupled plasma (ICP) operating at 13.56 MHz was used in this study. In general terms, the ICP functions as a single-turn secondary winding on a transformer. The rf-current in the flat coil antenna, Figure 1, generates an rf magnetic field which passes through a dielectric (in this case, quartz) window into the vacuum chamber/plasma volume, as shown. The time-varying magnetic field produces (via Faraday's law) electric field lines that form a single loop adjacent to the antenna. The electric field accelerates electrons to high energies, which in turn ionize and excite atoms to create the plasma, thus providing the primary means of electric power coupling to generate the plasmas. Capacitive coupling between the antenna and the plasma also occurs to a degree depending on plasma operating conditions, due to the high voltage applied to drive the antenna current.

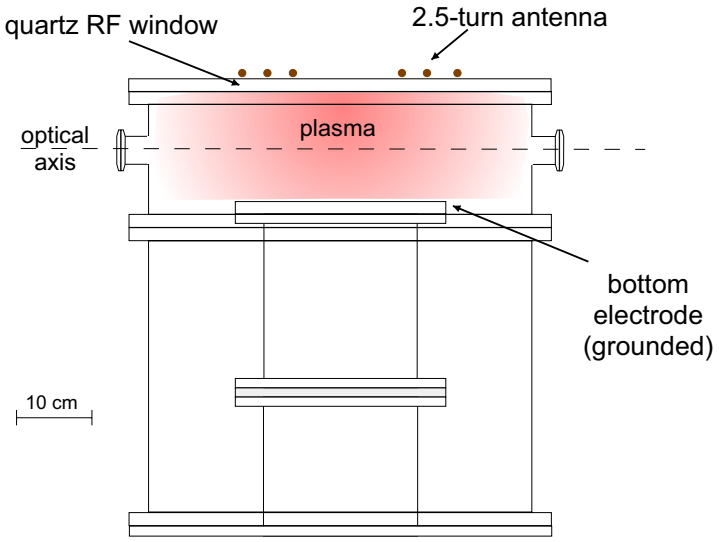

Figure 2: A cross-section of the plasma chamber.

A side view of the vacuum chamber is shown in Figure 2. The 50 cm diameter, Al-walled, vacuum chamber is evacuated with a 1000 1/s turbo pump backed by a 50 cfm dual-stage rotary-vane vacuum pump. The chamber base pressure is in the 10^{-6} Torr range. A mass flow controller is used to feed research grade oxygen (99.9999% purity) into the system at a fixed flow rate. The gas pressure in the chamber, which is measured by a 100 mTorr (full scale) capacitive manometer, is controlled with a throttle valve in the exhaust line.

The system includes a 30 cm diameter, 2.5 turn, flat-coil ICP antenna adjacent to a quartz vacuum window. A 'pi' matching network is used for impedance matching between the 3 kW, 13.56 MHz power supply and the plasma. When optimally tuned for 1000 W forward power (reported by the power supply), the reflected power is typically 0-25 W for pressures above 10 mTorr and up to 120 W for pressures lower than 10 mTorr. The reflected power is highly dependent on the setting of the tuning capacitor and only weakly dependent on that of the load capacitor.

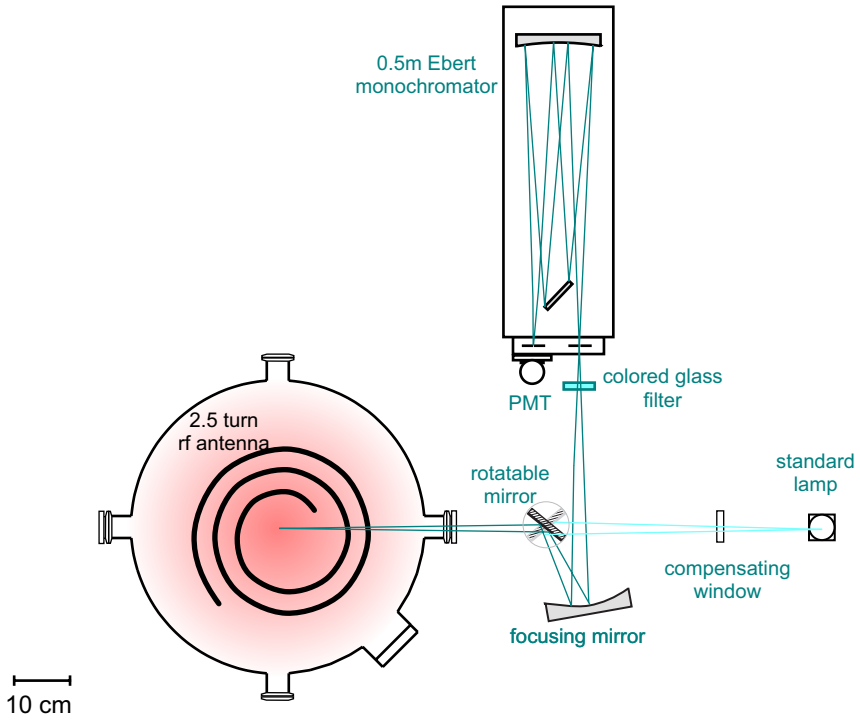

Figure 3: A top down view of the optical instrumentation and plasma chamber. Emitted light leaves the chamber at the view ports and is focused into the aperture of the monochrometer.

The optical system used for emission measurements is shown in Figure 3. This system uses a 0.5 meter monochromator in conjunction with a PMT to examine a single wavelength at a time. The PMT output is fed into an electrometer and the output is recorded by a computer as the monochromator is slowly scanned (12.5nm/min). Colored glass filters were used for order sorting and to reduce scattered light in the monochromator. Measurements were made with an effective resolution of 0.13 nm. A reference spectrum used to correct for the spectral sensitivity of the system makes use of a spectral irradiance standard lamp as a light source, connected to the optical path when needed by pivoting a rotatable mirror.

Spectra were also recorded with a Verity SD1024FH spectrograph which has an effective resolution of ~1.4 nm. Unfortunately, the O^+ emission peaks are very small and easily hidden by nearby molecular emissions. With the high resolution scanning monochromator, it was generally possible to extract the narrow O^+ peaks from the broad molecular emissions, but it was impossible to identify the O^+ emissions with the lower resolution spectrograph.

Experimental procedure

Preliminary spectra: A series of three spectra were taken under conditions that cover the range of operating conditions, for the purpose of identifying suitable O, O_2, O^+, and O_2^+ emission lines The ICP was first operated at 600 W and 15 mTorr Ar for 30 minutes in a "discharge cleaning" step. Next, the Ar was evacuated from the chamber and 7 sccm O_2 gas was introduced. The three spectra were recorded in 100 to 400 nm blocks (depending on the glass filter used for that range) from 310 to 800 nm for the following conditions: 1) 600 W (forward minus reflected

power) ICP power and 15 mTorr O_2, b) 1500 W ICP power and 5 mTorr O_2, and c) 1500 W ICP power and 2.5 mTorr O_2. Each spectrum was scanned at a speed of 125 Å/min which is ~45 min per spectrum.

Spectral feature identification: The tedious task of identifying features in the spectra is simplified with the information from the NIST website (for O and O^+) [1] and the *Tables of Spectral Lines of Neutral and Ionized Atoms* by Striganov and Sventiskii (for O, O^+, O_2, and O_2^+)[2], which both have listed the emissions of O and their respective wavelengths. The 1500 W, 2.5 mTorr spectrum, shown in Figure 4, was the most interesting case because these were the conditions under which the O^+ peaks were the most distinguishable. Take note that peaks of Cr also appear around ~360 nm and ~425 nm in Figure 4(a) and (b) The source of the Cr present in the plasma is presumed to be the stainless steel ground electrode (see Figure 2).

Once the spectral features were identified (Figure 4), a set of the peaks representative of the four species of interest were chosen for inclusion in a subsequent, more detailed study of pressure and power dependence. The selected peaks/bands for the respective species include: O^+ (397.33 nm and 441.49 nm), O_2^+ (~525 nm and ~555 nm), O (394.75 nm and 777.19 nm), and O_2 (~759). The plots shown in Figure 4 are subsets of a larger spectrum (310 nm – 900nm) that include the selected lines. The labels on the peaks selected for analysis are circled, with the exception of O_2 (759.37 nm), which is too small compared to O (777.19 nm) to be seen on the same plot. To more easily distinguish between different species' emissions, a color code has also been applied to the labeling of each emission. O^+ emissions are cyan, O_2^+ emissions are green, O emissions are black, O_2 emissions are red, and Cr emissions are gray.

Line intensities for different plasma conditions: The main set of experiments, described in the next section, focused on these seven peaks over a range of operating parameters: net (forward minus reflected) ICP power ranged from 500 to 2000 W in 500 W increments and O_2 pressure ranged from 1 to 30 mTorr. Intensities were recorded only for 10 nm blocks around each of the selected wavelengths of interest, in order to speed up data collection (compared to recording the full spectrum).

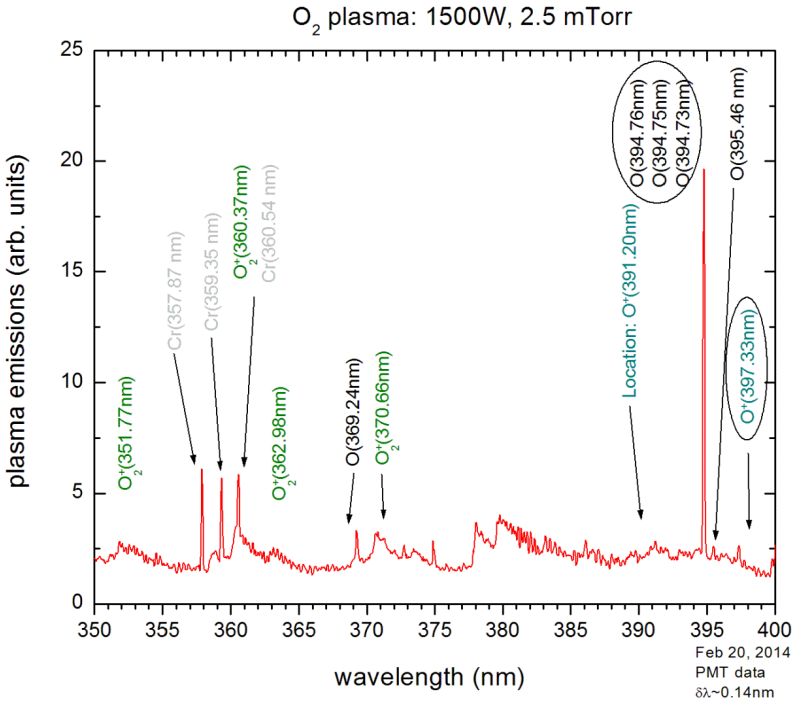

Figure 4 (a) O_2 plasma emission spectrum, 1500 W, 2.5 mTorr, 350-400nm

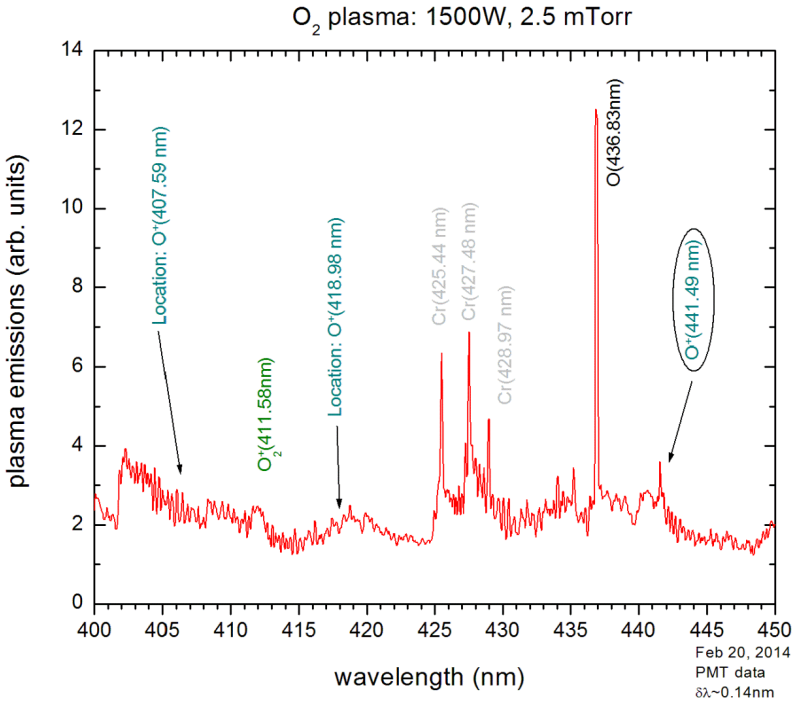

Figure 4 (b) O_2 plasma emission spectrum, 1500 W, 2.5 mTorr, 400-450 nm.

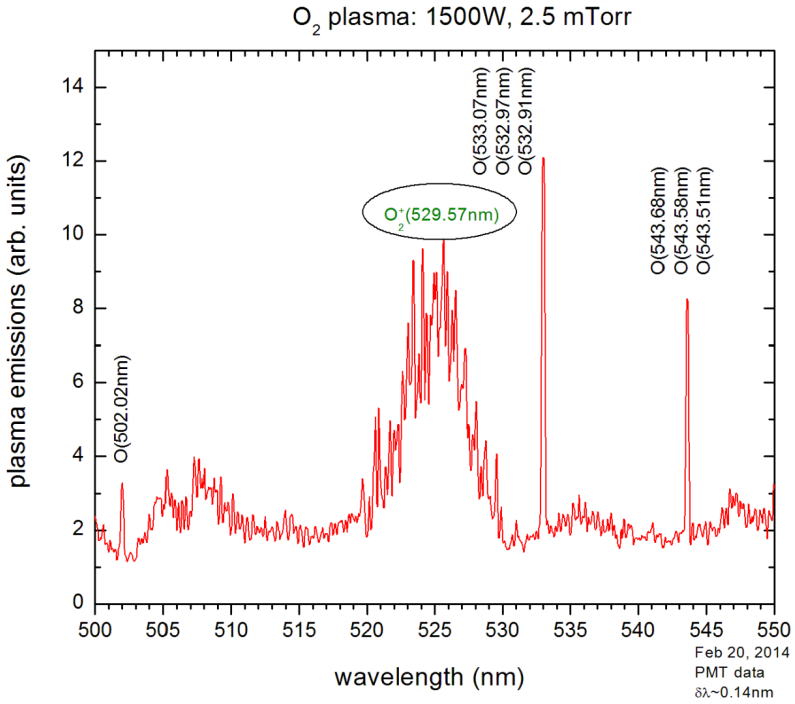

Figure 4 (c) O_2 plasma emission spectrum, 1500 W, 2.5 mTorr, 500-550 nm.

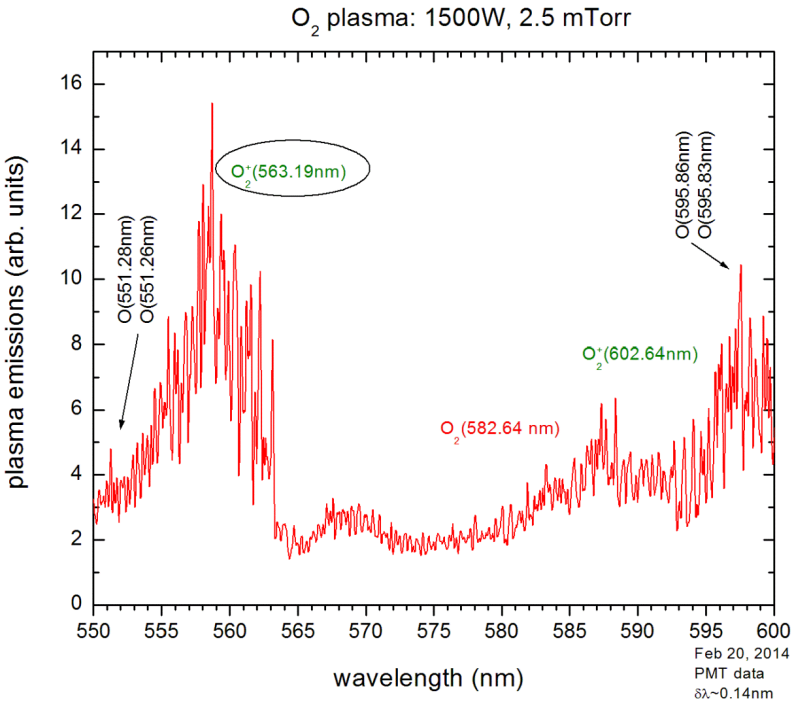

Figure 4 (d) O_2 plasma emission spectrum, 1500 W, 2.5 mTorr, 550-600 nm.

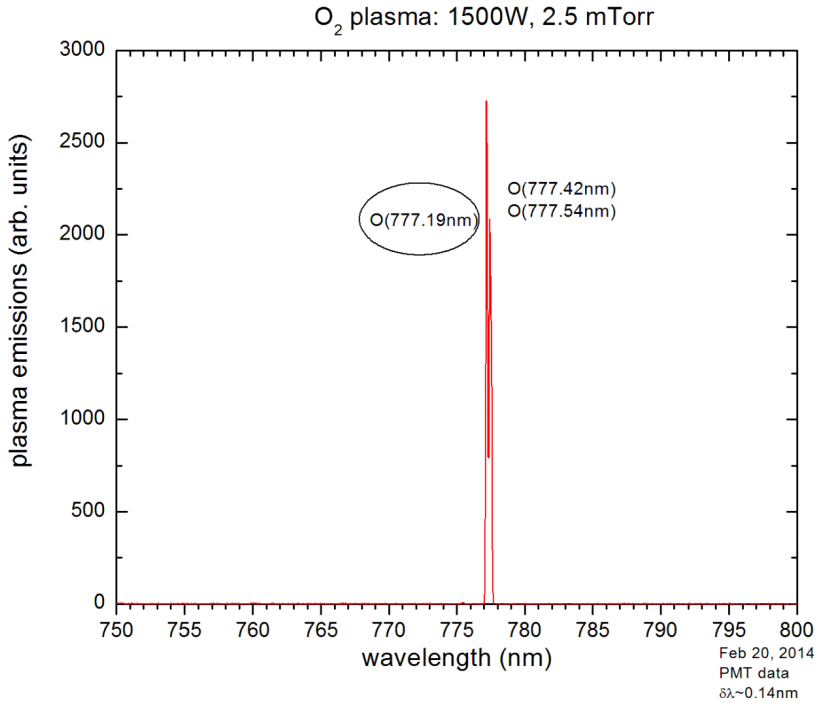

Figure 4 (e) O_2 plasma emission spectrum, 1500 W, 2.5 mTorr, 750-800 nm

A list of oxygen plasma emissions observed (including those in sections of the spectrum not depicted in Figure 4), is presented in Table 1. For each entry, wavelength and upper and lower electronic energy levels associated with the transition are provided. In addition, threshold energies from O, O_2, and O^+ ground state levels, respectively, are included as relevant.

Table 1. Emissions from oxygen plasma

Species	obs?	obs peak (nm)	component λ (nm)	component transition	E_{th} for O_2 (eV)	E_{th} for O (eV)	E_{th} for O^+ (eV)
O_2	YES	755-765	759.37	$B\ ^1\Sigma_g \rightarrow X\ ^3\Sigma_g$ (0-0)	2		
O_2^+	spec	370-373	370.66	$A\ ^2\Pi_u \rightarrow X\ ^2\Pi_g$ (1-8)	18		
	spec	410-413	411.58	$A\ ^2\Pi_u \rightarrow X\ ^2\Pi_g$ (0-9)	18		
	YES	515-530	529.57	$b\ ^4\Sigma_g^- \rightarrow a\ ^4\Pi_u$ (2-0)	18.5		
			527.47	(3-1)			
			525.92	(4-2)			
			525.12	(5-3)			
			524.10	(6-4)			
	YES	550-565	563.19	$b\ ^4\Sigma_g^- \rightarrow a\ ^4\Pi_u$ (1-0)	18.5		
			559.76	(2-1)			
			556.67	(3-2)			
			554.08	(4-3)			
			552.09	(5-4)			
O	YES	394.7	394.73	$4p\ ^5P_3 \rightarrow 3s\ ^5S_2$	17.4	12.28	
			394.75	$4p\ ^5P_2 \rightarrow 3s\ ^5S_2$			
			394.76	$4p\ ^5P_1 \rightarrow 3s\ ^5S_2$			
	(yes)	436.83	436.83	$4p\ ^3P_{2,1,0} \rightarrow 3s\ ^3S_1$	17.5	12.36	
	(yes)	533	532.91	$5d\ ^5D_{2,1,0} \rightarrow 3p\ ^5P_3$	18.2	13.06	
			532.97	$5d\ ^5D_{3,2,1} \rightarrow 3p\ ^5P_3$			
			533.07	$5d\ ^5D_{4,3,2} \rightarrow 3p\ ^5P_3$			
	(yes)	544	543.52	$6s\ ^5S_2 \rightarrow 3p\ ^5P_1$	18.1	13.02	
			543.58	$6s\ ^5S_2 \rightarrow 3p\ ^5P_2$			
			543.69	$6s\ ^5S_2 \rightarrow 3p\ ^5P_3$			
	YES	777	777.19	$3p\ ^5P_3 \rightarrow 3s\ ^5S_2$	15.8	10.74	
			777.42	$3p\ ^5P_2 \rightarrow 3s\ ^5S_2$			
			777.54	$3p\ ^5P_1 \rightarrow 3s\ ^5S_2$			
	spec	845	844.62	$3p\ ^3P_0 \rightarrow 3s\ ^3S_1$	16.1	10.99	
			844.64	$3p\ ^3P_2 \rightarrow 3s\ ^3S_1$			
			844.68	$3p\ ^3P_1 \rightarrow 3s\ ^3S_1$			
O^+	YES	397.33	397.33	$3p\ ^2P_{3/2} \rightarrow 3s\ ^2P_{3/2}$	45.3	40.2	26.56
	YES	441.49	441.49	$3p\ ^2D_{5/2} \rightarrow 3s\ ^2P_{3/2}$	45.0	39.9	26.25

Observation key:
YES = Peaks already tabulated for full 1-30 mTorr, 500-2000W set.
(yes) = Spectra recorded for full 1-30 mTorr, 500-2000W set, *but* peak areas have not (yet) been extracted.
spec = Observed in the three survey spectra, but were not recorded for full set of plasma conditions.

Threshold energies for disassociative excitation processes from the O_2 g.s. are theoretical onset energies only and do not include the kinetic energies of O, O^+ atoms/ions.

In Actinometry measurements of the atomic O density, the 845nm is preferred over the 777nm line since the 777nm line is mainly produced by disassociative excitation of O_2, whereas the 847nm line includes a large contribution from atomic excitation.

Determination of peak area: For each emission peak, the intensity was determined as the area under the peak multiplied by the wavelength dependent correction factor. Calculating the area of the O_2^+, O, and O_2 peaks or bands is straightforward, while computing the area of the O^+ peaks required extra care due to its weak intensity. For the first three, standard computational software was used to either numerically integrate the area under an entire emission band in the case of neutral or ionized oxygen *molecules* and atomic oxygen lines with overlapping triplets (listed as "component wavelengths" in Table 1, or to fit a Gaussian (isolated atomic oxygen lines), from which the area can be readily calculated. However, the calculation is more difficult in the case of the O^+ peaks. The relative intensities are very low compared to the other species and thus the signal to noise ratio is very low. An extra step is needed to calculate the area. Consider the example shown in Figure 5:

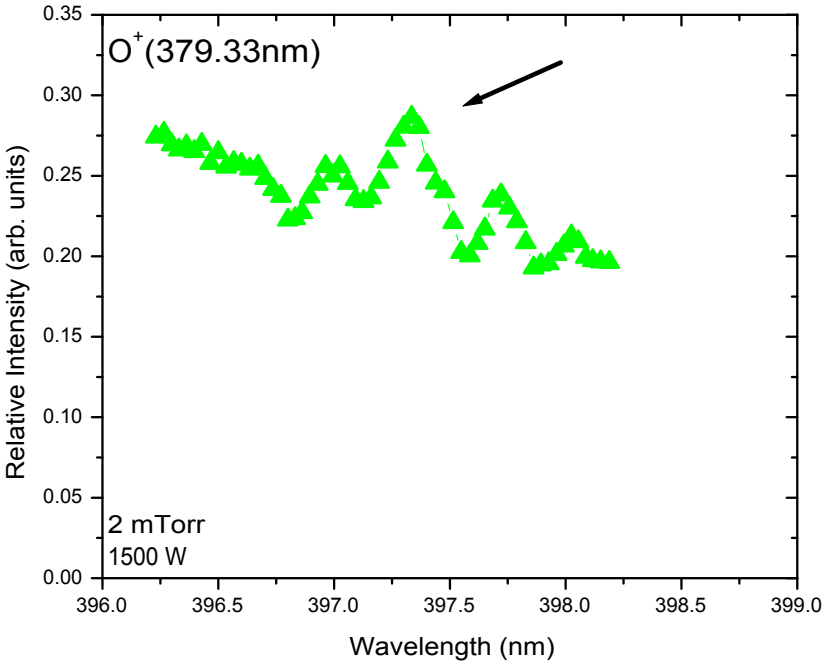

Figure 5: The section of the spectrum from 396 to 398 nm, taken at 1500 W and 2 mTorr shows the small amplitude of the O^+ (397) peak (identified with a black arrow) relative to the background spectrum.

Figure 5 shows a sample of the spectrum focusing around the O^+ peak at 397.33 nm. There is a linear trend to the background data in the vicinity of the peak. A linear function is fit to the background and then subtracted from the data to establish a base for the peak. A Gaussian is fit to the peak following baseline subtraction, and is used to compute the peak area.

Data and Discussion:

Ion species: Figures 6 and 7 show that for a given power, the intensities of O^+ (397 nm) and O_2^+ (555 nm and 525 nm) peak at or below 5 mTorr and then decrease with further increases in pressure. Data was not analyzed for O^+ at higher pressure (> 10 mTorr) because the signal to noise ratio for those cases was too low to extract peak areas.

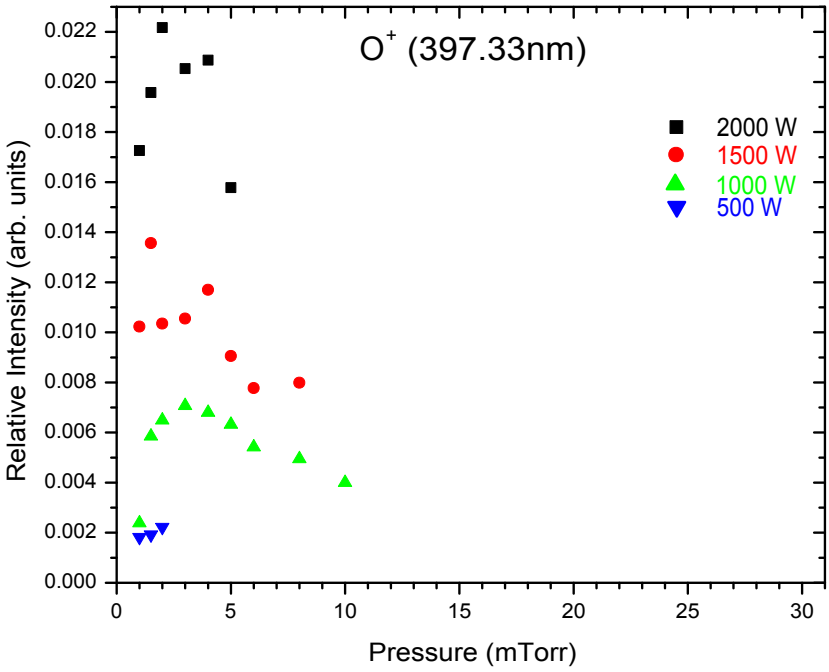

Figure 6(a). Intensity of the O^+ line (397.33 nm) versus pressure for different values of ICP power. Intensities are not plotted for conditions for which the signal to noise ratio was so low that reasonable estimation of the peak baseline was not possible.

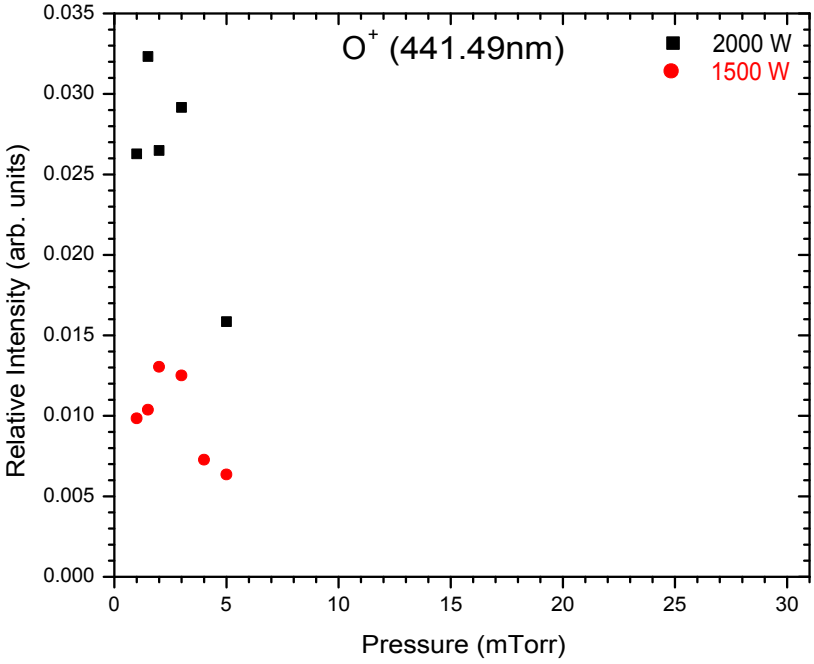

Figure 6(b). Intensity of the O^+ line (441.49 nm) versus pressure for different values of ICP power. Intensities are not plotted for conditions for which the signal to noise ratio was so low that reasonable estimation of the peak baseline was not possible.

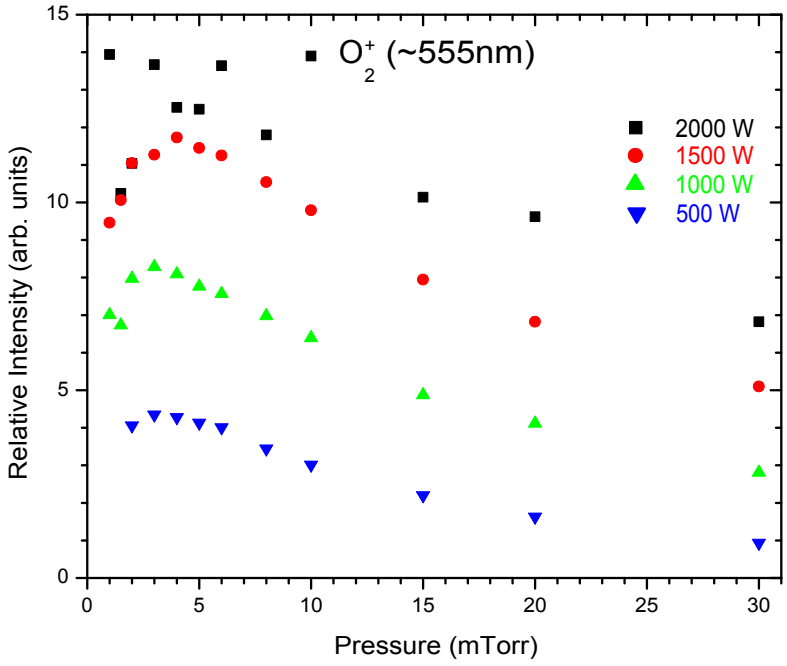

Figure 7(a). Intensity of O_2^+ bands, with band head at ~555 nm, versus pressure for different values of ICP power.

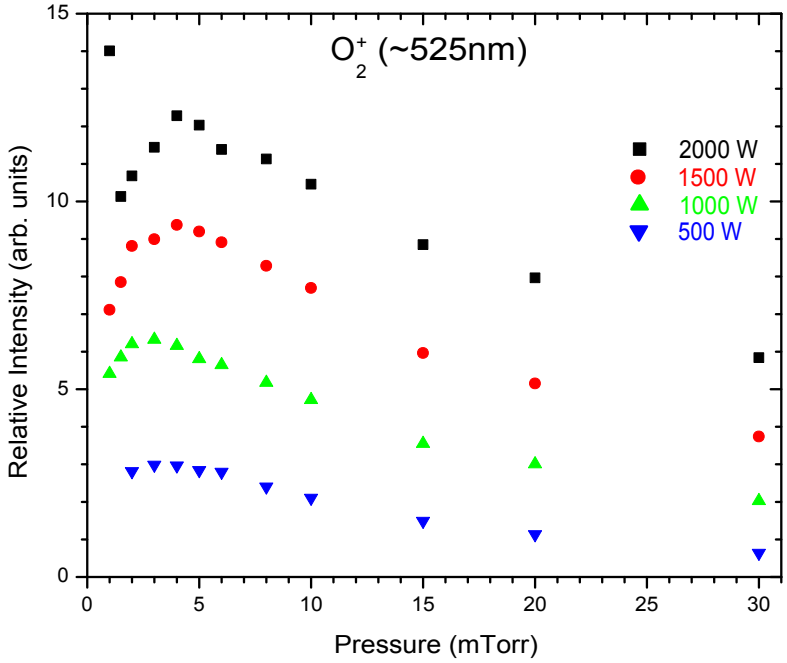

Figure 7(b): Intensity of O_2^+ bands, with band head at ~525 nm, versus pressure for different values of ICP power.

The electronically excited states that emit at the wavelengths shown in Figures 6 and 7 are populated through electron impact collisions, potentially with both neutral and ion species. For the intensities presented in Figures 6 and 7, the most probable pathway is electron collisions with *neutral* oxygen molecules. The excitation (and thus emission) rate is proportional to the concentrations of both collision partners, and is also proportional to a rate constant that depends

on the electron temperature The increase in intensity observed at low pressure can likely be attributed to concomitant increases in both electron density and ground state O_2 concentration, while at higher pressures, the concentration increases in these two species is overwhelmed by the declining reaction rate constant, due to falling electron temperature with pressure.

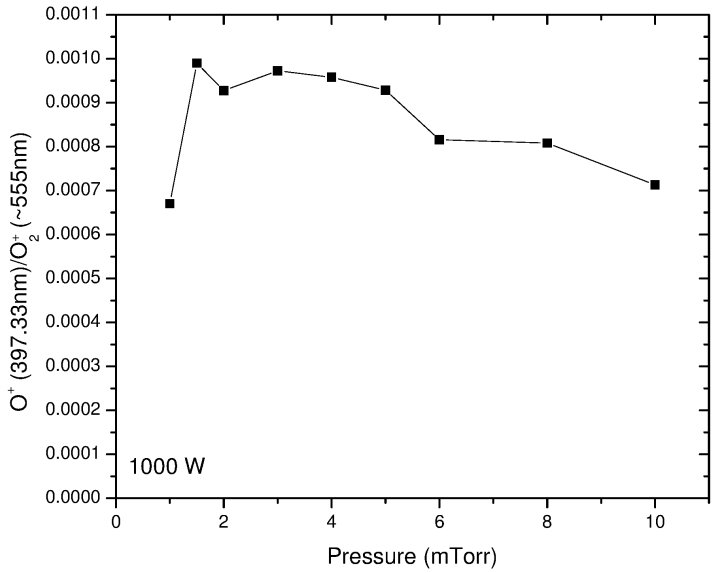

Figure 8: This graph shows the ratio of the intensities of the O^+ and O_2^+ emissions as a function of input power and pressure.

The intensity ratios for O^+ and O_2^+ for 1000 W and for pressures for which there was data are shown in Figure 8. The ratio of these two species remains fairly constant over the range of pressures. The species O^+ (397.33 nm) and O_2^+ (~555 nm) were chosen simply because they had larger emissions. There are other species of O^+ which were observed, although their emissions were not large enough to extract any data from their peaks.

Neutral species: Figures 9 and 10 contain plots of emissions from neutral species O and O_2, respectively.

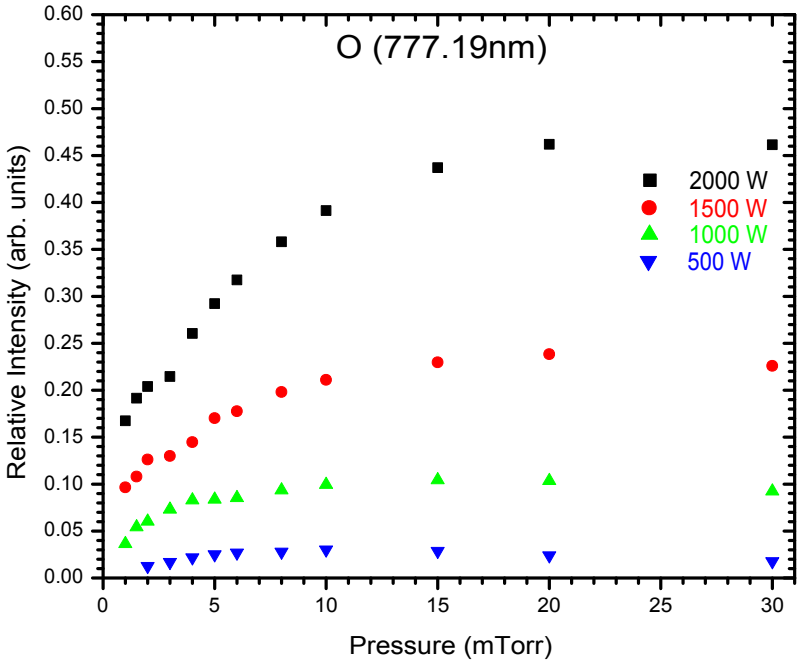

Figure 9 (a). Intensity of the O (777 nm) line versus pressure for different values of ICP power.

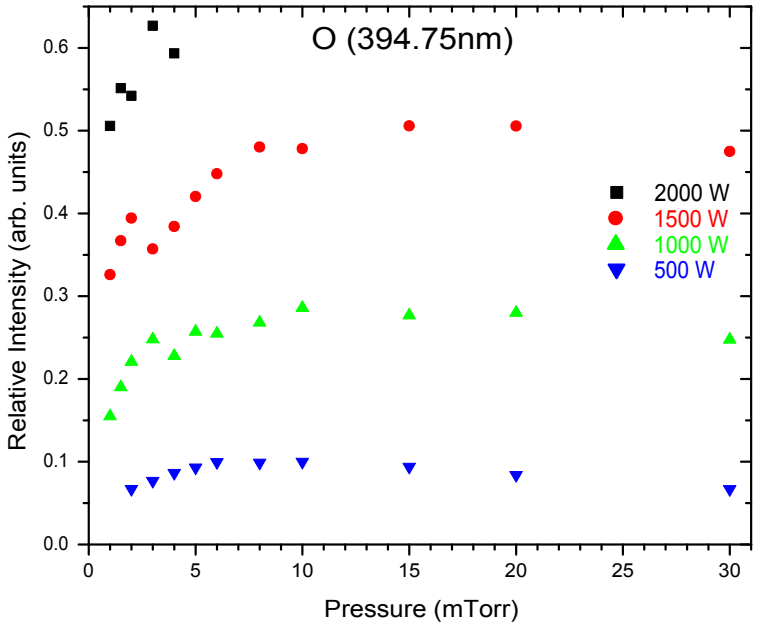

Figure 9 (b). Intensity of the O (395 nm) line versus pressure for different values of ICP power.

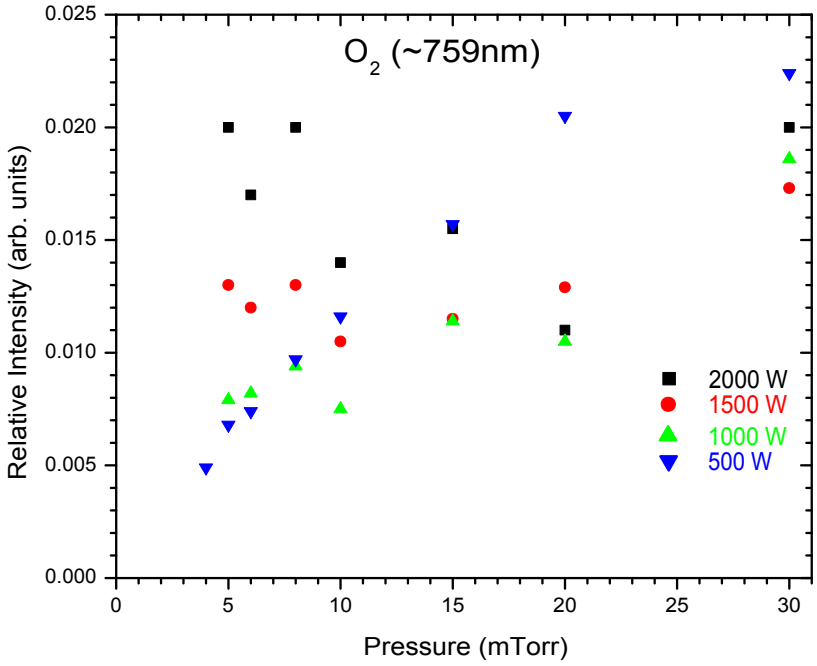

Figure 10. Intensity of the O_2 (~759 nm) line versus pressure for different values of ICP power.

In Figures 11 and 12, we present the ratios of ion emission intensities to those of the neutral atomic oxygen (777 nm) line intensity. In Figure 11 we see the ratio of intensity of the O^+ (397 nm) line to that of the 777 nm O line. Based on the likely scenario that both emitting states are populated primarily through dissociative ionization reactions between energetic electrons and neutral *molecular* oxygen, i.e., O_2, we expect the ratio to be independent of the concentrations of both collision partners, and thus to reflect the ratio of the rate constants for the two reactions, which in turn is, to lowest order, a function of electron temperature only. Figure 12 is presented in the same format, but shows the ratio of the (~555 nm) O_2^+ band to the same 777 nm O line. It is also expected that collisions between electrons and neutral O_2 dominate production of the emitting O_2^+ state, and we see a similar trend with pressure.

The hypothesis that these emission lines are dominated by electron collisions with O_2 is qualitatively supported by the observed trend of decreasing ratio with increasing pressure. For example, the ion density certainly increases with increasing pressure, so if excitation of ground state O^+ were the primary mechanism for populating the emitting state for the 397nm ion line, we'd expect to see an increase in the ratio (or a more gradual decline) with pressure, in contrast to the results shown in Figure 11. Furthermore, the electron energy thresholds for the two dissociative excitation reactions to produce O^{+*} and O^*, respectively, differ by nearly a factor of three (45.3 eV vs. 15.8 eV, as seen in Table 1). Since the electron temperature is known to decrease with increasing pressure, it is reasonable to expect the rate constant for O^{+*} to fall off more rapidly with pressure than that for O* production, leading to the observed trend. At this point, however, this explanation is speculative and a quantitative analysis would be needed to verify the hypothesis.

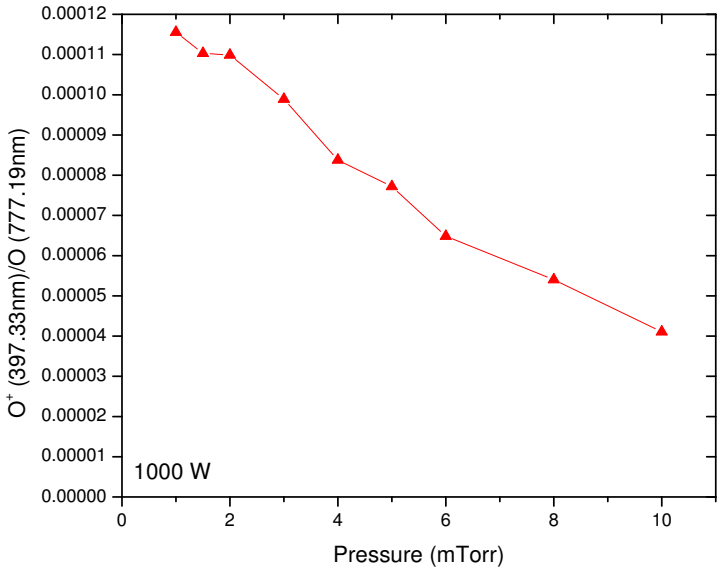

Figure 11. Line ratio versus pressure for different values of ICP power.

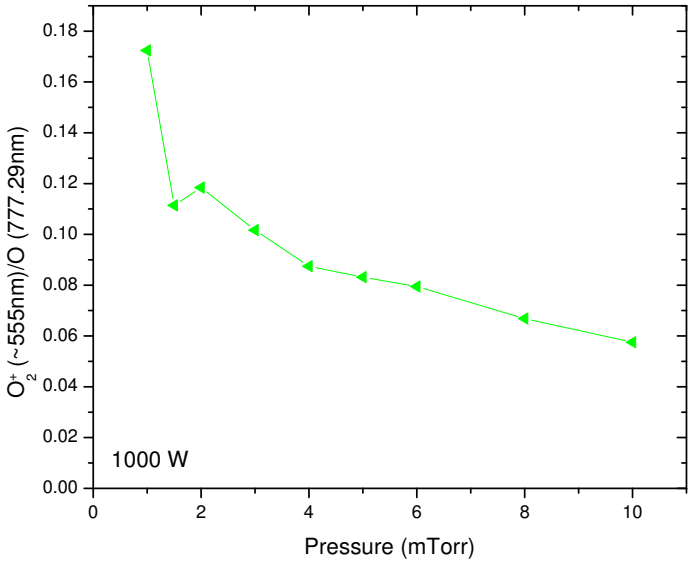

Figure 12. Line ratio versus pressure for different values of ICP power.

Concluding remarks

It would be interesting to observe the plasma run over a wider range of plasma parameters, but our system has limitations. One of the most re-occurring problems experienced is the high reflected power at low pressures. This was frustrating in the data collection because it was under these situations where the ion intensities peaked. The high reflected power sometimes caused the

rf-power supply to overheat and turn off. This was overcome by letting the system cool before taking data at low pressures. This becomes more of a problem as the forward power is increased, which is why we decided to use a maximum of only 2000 W.

We were able to observe O^+ and O_2^+ peaks and we have observed that their intensities peak at low pressure conditions. Since the intensity ratio of the two ions varied little with the plasma parameters over this range of input power and pressure, we can infer that the excitation rates into the upper excited states O^+* and O_2^+* do not vary much with plasma conditions. Nevertheless, if both excited ions are primarily produced by electron-impact ionization of O_2 (as compared to excitation of ground state O^+ and O_2^+ ions), this may only tell us that the creation rates for both ions are the same. Indeed, if the lifetimes of the two ions are quite different (i.e., their recombination rates or wall loss rates are different), the abundances of O^+ and O_2^+ may be quite different.

References

[1] NIST ASD Team, Y. Ralchenko, A. E. Kramida, and J. Reader, NIST Atomic Spectra Database (version 3.1.5), [Online]. Available; physics.nist.gov/PhysRefData/ASD/lines_form.html, 2010. National Institute of Standards and Technology, Gaithersburg, MD.

[2] A. R. Striganov and N. S. Sventitskii, Tables of Spectral Lines of Neutral and Ionized Atoms, IFI/Plenum, New York, 1998.